Thin-Walled Structures 131 (2018) 336–346

Contents lists available at ScienceDirect

Thin-Walled Structures

journal homepage: www.elsevier.com/locate/tws

Full length article

Buckling analysis of an inflated arch including wrinkling based on Pseudo Curved Beam model

Z.M. Xue[a,b], C.G. Wang[a,b,*], J.T. Kang[a,b], H.F. Tan[a,b]

[a] Center for Composite Materials, Harbin Institute of Technology, Harbin 150080, China
[b] National Key Laboratory of Science and Technology on Advanced Composites in Special Environments, Harbin Institute of Technology, Harbin 150080, China

ARTICLE INFO

Keywords:
Inflated arch
Buckling
Wrinkling
Pseudo Curved Beam
Stiffness modification

ABSTRACT

A Pseudo Curved Beam (PCB) model is proposed to analyze the buckling behaviors of inflated arch. The wrinkling (local buckling) effect is considered in the PCB model by modifying the cross-sectional area and sectional moment of inertia in the stiffness matrix. The wrinkling angle, wrinkling and failure load are then predicted based on the proposed PCB model. The bending experiment and numerical simulation of a quarter-circle inflated arch are performed to verify the validation of the PCB model. The effects of load conditions, constraint conditions, structural geometric parameters, inflation pressure and material properties on the buckling characteristics of inflated arch are parametrically studied in the end. The method and results provide good references for the load-carrying design of inflated structures.

1. Introduction

Inflatable membrane structures, due to their ease of portability, low packed volume, and light weight, have been used as main load-carrying members in civilian structures and aeronautical structures [1–4]. The inflated membrane can carry compressive stress produced by external loads and will restore its initial shape after being overloaded, because generally the load-induced membrane stresses are well below the membrane strength [5–7].

However, the complex wrinkling effect, which plays a crucial role in deformation process, makes the theoretical predictions on buckling characteristics of inflated structures extremely difficult. The statics behaviors (e.g. load-deflection behavior, buckling behavior) [5–13], the dynamic deployment performance [13], vibration characteristics [14–16] of inflated torus, arch and air-inflated frame were analyzed mainly based on experiments and numerical simulations. The theoretical works have been carried out to illuminate the mechanical behaviors of the inflated membranes, such as the global buckling, local wrinkling behavior [17,18] and the cross-sectional ovalization (also named as "Brazier effect") [19–21]. Comer and Levy [22] modeled the bending behavior of an inflated beam based on the Euler-Bernoulli's kinematics. Fichter [23] derived nonlinear equilibrium equations of inflated beam under bending based on the Timoshenko's kinematics and the principle of minimum potential energy. George [13] analyzed the in-plane and out-of-plane buckling characteristics of inflated ring based on the virtual work principle. The ovalisation and bifurcation instabilities of cylinders in pure flexure were studied by Wadee et al. [19,20] using a hoop second-degree trigonometric series solution. Le van and Wielgosz [24] improved Fichter's theory [23] to consider the interactive bending and buckling behaviors of inflatable beams by establishing the virtual work principle in three-dimensional Lagrangian form. David's et al.[25,26]developed a Timoshenko beam element based on the virtual work principle, which includes pressure effects, wrinkling, and geometric nonlinearities, to analyze the bending behavior of pressurized fabric beams. Then they developed the quadratic Timoshenko beam element to consider the material and geometrical nonlinearity of inflated arch, and a semicircular inflated fabric arch were tested to verify the beam-element models [5]. Brayley et al.[10] developed a beam finite-element model, which incorporates the braid angle and strap stiffness, to study the bending behaviors of the inflated, braided, strapped beams and arches. Wang et al. [27]proposed a Pseudo-beam method based upon Fichter's theory and the virtual work principle with a 3-node Timoshenko's beam model. The concept of the wrinkling factor was then proposed to predict the critical wrinkling load and initial wrinkling location of inflated beam under bending [28].

In general, the application of shell element in wrinkling analysis results in time consuming and convergence difficulty. Neither Euler nor Timoshenko beam is capable of explaining the bending-twisting and/or extension-twisting couplings which truly exists in the deformation process of curved beam [29–33]. Thus, it is necessary to use the curved

* Corresponding author at: Center for Composite Materials, Harbin Institute of Technology, Harbin 150080, China.
E-mail address: wangcg@hit.edu.cn (C.G. Wang).

https://doi.org/10.1016/j.tws.2018.06.044
Received 2 December 2017; Received in revised form 16 May 2018; Accepted 29 June 2018

Nomenclature

s	curvilinear coordinate
$\mathbf{r}_{P0}$	position vector of the point P_0
$\mathbf{x}$, $\mathbf{y}$, $\mathbf{z}$	rectangular Cartesian coordinates
λ	tangent vector
κ	curvature
$\mathbf{t}(s)$, $\mathbf{n}(s)$, $\mathbf{b}(s)$	Frenet-Serret frame
$\mathbf{e}_s$, $\mathbf{e}_y$, $\mathbf{e}_z$	cross-section curvilinear spindle coordinates
χ	angle between the spindle coordinate system and the Frenet-Serret frame
$\mathbf{e}$, $\hat{\mathbf{e}}$, $\mathbf{e}^*$	cross-section spindle coordinate system at the initial configuration, deformed configuration and deformation configuration based on Kirchhoff Hypothesis
θ_1, θ_2, θ_3	rotations of $\mathbf{e}$ in the directions of $\mathbf{e}_s$, $\mathbf{e}_y$ and $\mathbf{e}_z$ respectively
$-\gamma_2$, $-\gamma_3$	rotations of $\mathbf{e}^*$ in the directions of $\mathbf{e}_s$, $\mathbf{e}_y$ respectively
x^1, x^2, x^3	local Cartesian coordinates
$\mathbf{i}^1$, $\mathbf{i}^2$, $\mathbf{i}^3$	unit vectors of local Cartesian coordinates x^1, x^2, x^3
R	radius of inflated torus
r	radius of cross-section of inflated torus
t	membrane wall thickness
p	inflation pressure
E	Young modulus
v	Poisson ratio
σ_r, σ_θ, σ_z	radial stress, circumferential stress and axial stress
A	cross-sectional area of inflated curved beam
I	area moment of inertia of inflated curved beam
J	area polar moment of inertia of inflated curved beam
σ_m, σ_0	maximum stress and minimum stress in axial direction
σ_{cr}	critical wrinkling stress of membrane
θ_w	wrinkling angle

Subscripts:

ϕ	initial state
0	current state

beam model to perform the buckling and wrinkling analysis of curved inflated beam. Based on this consideration, a Pseudo Curved Beam (PCB) model is proposed to analyze efficiently the wrinkling and buckling characteristics of the inflated arches in this paper. The paper is structured as follows. In Section 2, the Pseudo Curved Beam model is derived at first. The wrinkling effect is also considered in the PCB model by modifying the cross-sectional area and sectional moment of inertia in the stiffness matrix. In Section 3, the mechanical characteristics of a quarter circle inflated arch under bending are experimental tested and numerically simulated. In Section 4, the results obtained from experiments and simulations are used to verify the validation of proposed PCB model. In Section 5, the effects of load conditions, constraint conditions, structural geometrical parameters, inflation pressure and material parameters on structural buckling load of inflated arch are studied to provide references to design the load-carrying capacity of inflated structures. The conclusions are drawn in the end.

2. Pseudo Curved Beam model

2.1. Curved beam model

The arch-type structure is a typical naturally curved structure. A large number of straight beam (Bernoulli-Euler Beam or Timoshenko beam) elements are generally used to model the curved or twisted structures. The accurate results can be obtained when the number of straight beam elements is large enough, which will make the computation time-consuming [30]. On the other hand, the straight beam element itself, however, is incapable of illuminating adequately the mechanical characteristics of the curved structure, such as arch, due to the bending-twisting and/or extension-twisting couplings existing in curved structure deformation process. In this section, we deduce the geometric equation of a curved beam and establish the curved-beam element model.

2.1.1. Geometric configuration

The geometric configuration of space arbitrary curved beam is shown in Fig. 1. An arbitrary point P_0 is set on the center axis of curved beam. The parameter s represents arc length from the curved origin to point P_0 along the center axis.$\mathbf{r}_{P0}$ is the position vector of the point P_0 in a three-dimensional global coordinate system $\mathbf{x}$, $\mathbf{y}$, $\mathbf{z}$.

The central axis tangent vector and the curvature are defined as [31,32]

$$\boldsymbol{\lambda}(s) = \frac{d\mathbf{r}_{P0}}{ds} \quad \kappa(s) = \left|\frac{d\lambda}{ds}\right| \tag{1}$$

Two mutually orthogonal unit vectors $\mathbf{n}(s)$ (main normal vector) and $\mathbf{b}(s)$ (binormal vector) define the cross-sectional plane of curved beam. Therefore $\mathbf{t}(s)$, $\mathbf{n}(s)$, $\mathbf{b}(s)$ constitute the Frenet-Serret frame, and

$$\mathbf{t}(s) = \boldsymbol{\lambda}(s) \quad \mathbf{n}(s) = \frac{1}{\kappa}\frac{d\lambda}{ds} \quad \mathbf{b}(s) = \boldsymbol{\lambda}(s) \times \mathbf{n}(s) \tag{2}$$

The torsion at P_0 is defined as

$$\tau(s) = \frac{d\mathbf{b}(s)}{ds} \tag{3}$$

A spindle coordinate system $\mathbf{e}_s$, $\mathbf{e}_y$, $\mathbf{e}_z$ are introduced to facilitate the derivation of Green Strain tensor in next section. The spindle coordinate system has its origin on the axis of beam, and its unit vector $\mathbf{e}_s$ is in the tangent direction of beam. The parameter χ represents the angle between the spindle coordinate system and the Frenet-Serret frame (Fig. 1). The relation between these two coordinate systems is given by

$$\begin{bmatrix}\mathbf{e}_s\\ \mathbf{e}_y\\ \mathbf{e}_z\end{bmatrix} = \begin{bmatrix}1 & 0 & 0\\ 0 & \cos\chi & \sin\chi\\ 0 & -\sin\chi & \cos\chi\end{bmatrix}\begin{bmatrix}\mathbf{t}\\ \mathbf{n}\\ \mathbf{b}\end{bmatrix} \tag{4}$$

then differentiation of Eq. (4) based on Frenet-Serret formulas yields

$$\begin{bmatrix}\mathbf{e}_{s,s}\\ \mathbf{e}_{y,s}\\ \mathbf{e}_{z,s}\end{bmatrix} = \begin{bmatrix}0 & \kappa_3 & -\kappa_2\\ -\kappa_3 & 0 & \kappa_1\\ \kappa_2 & -\kappa_1 & 0\end{bmatrix}\begin{bmatrix}\mathbf{e}_s\\ \mathbf{e}_y\\ \mathbf{e}_z\end{bmatrix} = \mathbf{K}_s\begin{bmatrix}\mathbf{e}_s\\ \mathbf{e}_y\\ \mathbf{e}_z\end{bmatrix} \tag{5}$$

Where

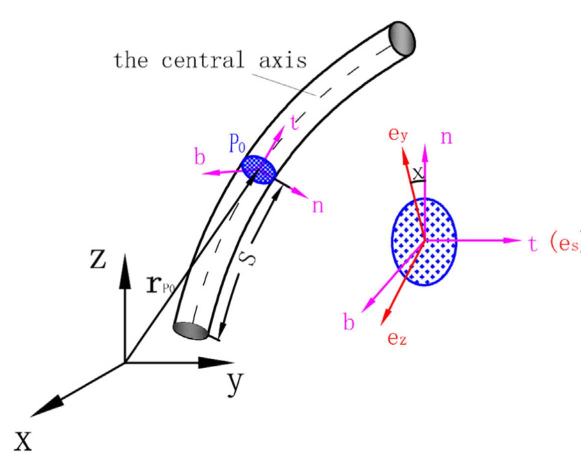

Fig. 1. Space arbitrary curved beam.